APPLIED ORGANOMETALLIC CHEMISTRY
Appl. Organometal. Chem. 2007; **21**: 211–217
Published online in Wiley InterScience
(www.interscience.wiley.com) DOI:10.1002/aoc.1210

Bioorganometallic Chemistry AOC

The synthesis, crystal structures and SOD activities of a new ligand (L^{se}) and $Co(L^{se})_2(SCN)_2$ complex [L^{se} = selenium ether bis-(*N*-1-methyl- benzotriazole)]

Yanchun Lu, Yu Tang, Hong Gao, Zhihui Zhang* and Haifeng Wang

The College of Chemistry, Nankai University, Tianjin 300071, People's Republic of China

Received 24 August 2006; Revised 24 December 2006; Accepted 1 January 2007

A new ligand containing selenium, Se (CH_2-*N*-Btrzole)$_2$ (L^{se}) (Btrzole = benzotriazole) and its cobalt(II) complex, $Co(L^{se})_2(SCN)_2$, have been synthesized and the molecular structures of the title compounds have been determined by X-ray techniques. The L^{se} is a *meso*-configuration with a symmetric plane through the Se center, the intermolecular weak interactions of Se–Se, Se–N and $\pi-\pi$ stacking between benzotriazole rings to extend the molecular structure to two-dimensional network configuration. In the Co(II) complex, the metal center is in a six-coordinated octahedral environment. Two Co(II) atoms are linked by two ligands to form a 20-membered macrocycle; the adjacent macrocycles are linked by coordinated bond of Co–$N_{bentrozole}$ to extend an infinite double strained chain. The SOD activity of the ligand and Co(II) complex have been studied by using the pyrogallol autoxidation method; thermal properties and luminescent properties of Co(II) complex have been tested, and the details of those properties have been discussed. Copyright © 2007 John Wiley & Sons, Ltd.

KEYWORDS: selenium ether; benzotriazole; Co (II) complex; crystal structure; SOD activity

INTRODUCTION

The chemistry of selenium has been received much attention because of its potential applications in various fields. For example, selenium compounds as the synthetic auxiliary are used in organic reactions,[1–3] the selenium compounds present excellent biological activities,[4] and the selenium compounds are used as single-source precursors in syntheses of binary and ternary metal chalcogenides.[5–11] However, most reports concern the organoselenium compound, and the coordination of selenolates as a ligand has not been widely studied. The metal complexes with ligands containing selenium and nitrogen donors are interesting for several reasons:[12] first, they can provide insight into the competitive coordination behavior between the hard and soft Lewis basic nitrogen and selenium towards the same metal center; and second, whether the biological activity of the selenium increases or not under the action of metal ions in the same compound and the interaction of selenium with metal ions in a same complex is a subject worth studying.

The benzotriazole and it derivatives are the versatile ligands in coordination chemistry.[13] The parent heterocycle on benzotirzole in its deprotonated form can coordinate with three metal ions and bridged link metal centers in *N*,*N*′-chelating model.[14,15]

In order to inspect the interaction of selenium with metal atoms in a same complex, we are currently engaged in the synthesis of new organoselenium as the ligand and study of the biological activity of the new ligand and its complex. Herein we report the crystal structure, spectral properties, and the super oxide dismutase (SOD) activity of new ligand containing selenium L^{Se} (Fig. 1) and its cobalt (II) complex.

EXPERIMENTAL

Materials and general methods

All chemicals were of analytical reagent grade. Solvents were purified according to the standard methods prior to use. Elemental analyses (C, H, N) were carried out

*Correspondence to: Zhihui Zhang, The College of Chemistry, Nankai University, Tianjin 300071, People's Republic of China.
E-mail: zhangzh67@nankai.edu.cn

Copyright © 2007 John Wiley & Sons, Ltd.

WILEY InterScience® DISCOVER SOMETHING GREAT

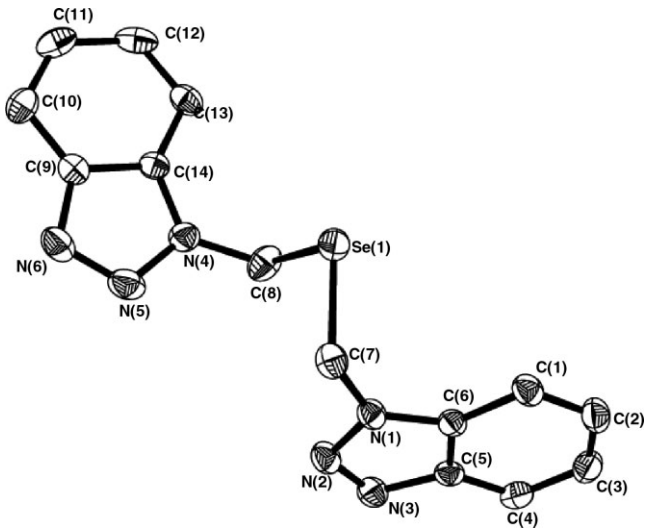

Figure 1. ORTEP diagram of Se (CH_2-*N*-Btrzole)$_2$ (L^{se}).

on a Perkin–Elmer analyzer model 240. IR spectra were recorded as KBr disks on a Shimadzu IR–408 infrared spectrophotometer in the region of 4000–600 cm^{-1}. UV–vis spectra were recorded on a Beckman DU–8B UV–vis spectrophotometer in the range 200–800 nm. Thermal stability (TG-DAT) was carried out on Netgzsch TG–209 thermal analyzer with a heating rate of 10 °C min^{-1} from room temperature to 800 °C. Fluorescence measurements were performed on a WGY-10 spectrophotometer. ^1H *NMR* spectra were recorded on a Varian Mercury VX 300 spectrometer at room temperature in DMSO[D6].

Synthesis of the ligand L^{Se}

The precursor 1-chloromethylbenzotriazole was prepared using modified literature methods.[16] A solution of 1-chloromethylbenzotriazole (6.70 g, 40 mmol) in CH_3OH (60 ml) was added to a solution of Na_2Se (2.50 g, 20 mmol) in H_2O (15 ml) with stirring at room temperature (r.t.) under a nitrogen atmosphere. A yellow precipitate appeared immediately. The mixture was stirred for 0.5 h at r.t., and then the temperature was increased to 70 °C. The reaction was kept at 70 °C for 2 h. The reaction mixture was filtered to remove the solvent. The crude products, earth-yellow powder, were obtained. The products were re-crystallized from CH_3OH and the straw yellow crystals of L^{Se} were isolated. Yield: 1.89 g, 55.2%. Calcd for $C_{14}H_{12}N_6Se$ (%): C, 48.98; H, 3.50; N: 24.49. Found (%): C, 48.87; H, 3.69; N, 24.16. ^1H NMR (300MHz, [D_6] DMSO): δ ppm, 7.456–8.080 (m, 8H, Phen-H); 6.214(s, 4H, CH_2). IR (KBr, cm^{-1}): 3016m, 2955s, 2660m, 2104m, 1610s, 1495s, 1452s, 1395m, 1304s, 751s. (m, medium; s, strong).

Synthesis of $[Co(L^{Se})_2(NCS)_2]_n$, 1

L^{Se} (68.8 mg, 0.20 mmol) was dissolved in $CHCl_3$ (5 ml) in a test tube. A solution of $CoCl_2 \cdot 6H_2O$ (23.8 mg, 0.10 mmol) in MeOH (3 ml) and a solution of KSCN (19.4 mg, 0.20 mmol) in MeOH (2 ml) were then added carefully in turn to the top of the L^{Se} solution without disturbing. The red single crystals of **1** suitable X-ray analysis were obtained after several weeks. Yield: 62%. Calcd for $C_{30}H_{24}CoN_{14}S_2Se_2$ (%): C, 41.82; H, 2.79; N, 22.77. Found (%): C, 41.76; H, 2.85; N, 22.69. IR (KBr, cm^{-1}): 3425(br), 2093(s, SCN), 1611(m, C═N), 1491(m), 1455 (s), 1392(w), 1309(s), 1215(s), 1083(s), 773(s), 742(s) (br, broad; s, strong; m, medium; w, weak).

X-ray crystallography

Crystals L^{Se} and $[Co(L^{Se})_2(NCS)_2]_n$ **1** were mounted on a glass fiber. Determination of the unit cell and data collection were performed using MoKα radiation (λ = 0.71073 ´Å) on a Bruker Smart 1000 diffractometer equipped with a CCD camera. The $\omega - \Phi$ scan technique was employed.[17] Semiempirical absorption corrections were applied using SADABS program.[18,19] The structures were solved primarily by direct methods and secondly by Fourier difference techniques and refined using the full-matrix least-squares method. The computations were performed with the SHELXL-97 program.[18,19] All non-hydrogen atoms were refined anisotropically. The hydrogen atoms were set in calculated positions and refined as riding atoms with a common fixed isotropic thermal parameter. Crystal parameters and structure refinements for the compounds are summarized in Table 1. Selected bond lengths and bond angles of L^{Se} and **1** are listed in Table 2.

SOD activity measurement

The SOD activities of L^{Se} and **1** were tested using the pyrogallol autoxidation method.[20,21] For the controlling test: Tris–HCl buffer (5 ml, pH = 8.2) was mixed with double distillated water (5 ml), and the mixture kept at 25 ± 0.2 °C for 20 min. To the mixture, 0.3 ml of pyrogallol solution (3 mmol dm^{-3}) in 0.1 mmol dm^{-3} HCl was added with stirring, and transferred to the cell for the absorption measurement at 325 nm on a Beckman DU-8B UV–vis spectrophotometer. The plots of absorptions vs time(s) were obtained and the slope of the line is the autoxidizing velocity of pyrogallol.

For the ligand and complex **1**: the solution of L^{Se} and **1** with various concentrations was kept at 25 ± 2 °C for 20 min, respectively. To every solution, 0.3 ml of pyrogallol solution (3 mmol dm^{-3}) was added and run using the same procedures as for pyrogallol samples. The plots on the absorption data of pyrogallol by the action of L^{Se} with various concentrations vs time (second) were made. The autoxidizing velocity of pyrogallol after adding the L^{Se} with various concentrations can be obtained from the slopes of the lines.

RESULTS AND DISSUSSION

The synthesis of L^{Se} and complex 1

The new ligand (L^{Se}) was synthesized in an oxygen-free atmosphere by employing a pure nitrogen providing method, because selenium powder is unstable in air and it is easily

Copyright © 2007 John Wiley & Sons, Ltd.

DOI: 10.1002/aoc

Table 1. Crystallographic data and structure refinements for L^{Se} and complex **1**

Complexes	L^{Se}	Complex 1
Empirical formula	$C_{14}H_{12}N_6Se$	$C_{30}H_{24}CoN_{14}S_2Se_2$
Formula weight	343.26	861.60
T (K)	293(2)	293(2)
Crystal size (mm)	0.28 × 0.22 × 0.16	0.22 × 0.16 × 0.12
Color	Colorless	Red
Crystal system	Monoclinic	Monoclinic
Space group	P2(1)/c	P2(1)/c
a (Å)	11.2064(12)	8.8224(7)
b (Å)	9.3363(10)	12.2997(9)
c (Å)	13.8543(15)	16.2659(12)
α (deg)	90	90
β (deg)	103.4240(10)	105.4280(10)
γ (deg)	90	90
V (Å^3)	1409.9(3)	1701.5(2)
Z	4	2
Calculated density (mg m^{-3})	1.617	1.682
Absorption coefficient (mm^{-1})	2.666	2.813
F (000)	688	858
θ range for data collection (deg)	2.65–25.03	2.10–25.03
Limiting indices	$-13 \le h \le 11$	$-10 \le h \le 9$
	$-11 \le k \le 11$	$-14 \le k \le 14$
	$-15 \le l \le 16$	$-14 \le l \le 19$
Reflections collected/unique	7429/2486	9117/3014
Data/restraints/params	2486/0/191	3014/0/224
Goodness-of-fit on F^2	1.067	1.035
Final R indices $[I > 2\sigma(I)]$	$R_1 = 0.0232$	$R_1 = 0.0235$
	$\omega R_2 = 0.0617$	$\omega R_2 = 0.0556$
R indices (all data)	$R_1 = 0.0274$	$R_1 = 0.0309$
	$\omega R_2 = 0.0641$	$\omega R_2 = 0.0581$
Largest difference peak and hole (e A^{-3})	0.381 and −0.488	0.437 and −0.361

oxidized to generate a red SeO_2. The generation of the bi-selenium or multi-selenium compounds should be avoided in the synthesis of L^{Se}, because bi-selenium and multi-selenium compounds have less solubility in normal solvents, such as methanol and chloroform. The new ligand, L^{Se}, is stable and soluble in common organic solvents. These behaviors make the compound an excellent ligand to study coordination reactions and biological activity through solution approaches.

The single crystals of $[Co(L^{Se})_2(NCS)_2]_n$ were obtained using the solvent diffusing method without disturbance, because the precipitate of the products is easily generated using the normal method.

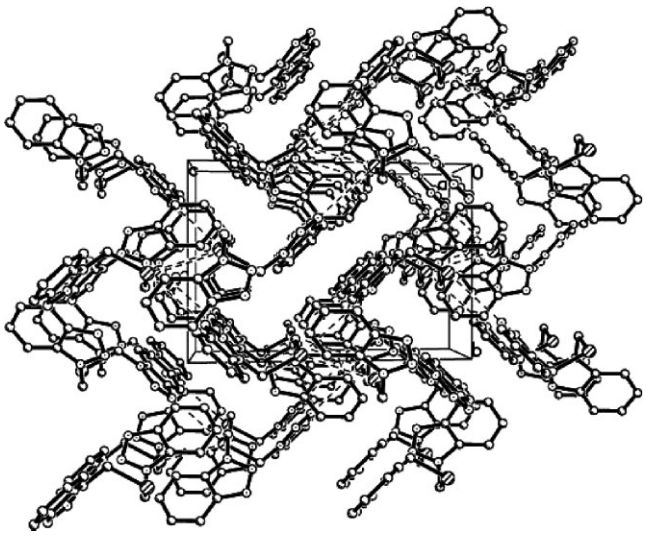

Figure 2. Two-dimensional network of L^{Se} formed by the $\pi-\pi$ interactions between benzotriazole rings.

X-ray structural characterization

The crystal of L^{Se}

A perspective view of L^{Se} is shown in Fig. 1. There is a symmetry-surface through the center Se atom, which presents a 1,1′-isomer. Two pendant arms, CH_2-*N*-Btrzole, on the selenium atom are *cis*-configuration with bond distances N(1)–C(7), N(4)–C(8), Se(1)–C(7) and Se(1)–C(8) of 1.434(3), 1.441(3), 1.952(2) and 1.956(2) Å, respectively. The ligand adopts a stretched out and twisted *anti-fac* conformation with a dihedral angle of 64.3° from two benzotriazole rings. The torsion angles of C(8)–Se(1)–C(7)–N(1) and C(7)–Se(1)–C(8)–N(4) are 67.25(15)° and 100.87(18)°, respectively.

There are weak interactions of Se···Se (3.840 Å) and N···Se (3.445 Å) in two L^{Se}, which extent the molecular structure to a two-dimensional network in the *ab* plane. The $\pi-\pi$ interactions between benzotriazole rings with a centroid–centroid distance of 3.887 Å stabilize the network further (Fig. 2).

Crystal of complex 1

The molecular structure of **1** is shown in Fig. 3(a). The Co(II) atom is in a six coordinated environment with four $N_{btrizole}$ atoms from L^{Se} and two N_{SCN} atoms being the axial positions, and four $N_{btrizole}$ atoms defining the equatorial plane. The bond length of Co–$N_{btrizole}$ is 2.1478 (16), 2.1478 (16), 2.2309 (17) and 2.2309 (17) Å, respectively, and the average of the bond length of Co–N_{NCS} is 2.0564(18) Å which is shorter than that of Co–$N_{btrizole}$, giving rise to a compressed octahedral configuration in which all the angles are close to the ideal ones. The Co–N bond lengths are quite similar to those of the known coordination polymer $[Co(bbbt)_2(NCS)_2]_n$ [Co–Nbbbt (av) = 2.218 Å, Co–N_{NCS} = 2.055(4) Å].[22] The

Copyright © 2007 John Wiley & Sons, Ltd.

DOI: 10.1002/aoc

Table 2. Selected bond lengths (Å) and angles (deg) for L^{Se} and **1**

L^{Se}			
Se(1)–C(7)	1.952(2)	Se(1)–C(8)	1.956(2)
N(1)–C(7)	1.434(3)	N(4)–C(8)	1.441(3)
C(7)–Se(1)–C(8)	96.56(10)	Se(1)–C(7)–H(7)[a]	109.1
Se(1)–C(7)–H(7)[b]	109.1	N(4)–C(8)–Se(1)	112.87(15)
Se(1)–C(8)–H(8)[a]	109.0	Se(1)–C(8)–H(8)[b]	109.0
Complex **1**			
Se(1)–C(8)	1.958(2)	Se(1)–C(7)	1.962(2)
Co(1)–N(7)[a]	2.0564(18)	Co(1)–N(7)	2.0564(18)
Co(1)–N(6)[b]	2.1478(16)	Co(1)–N(6)[c]	2.1478(16)
Co(1)–N(1)	2.2309(17)	Co(1)–N(1)[a]	2.2309(17)
N(7)[a]–Co(1)–N(7)	180.0	N(7)[a]–Co(1)–N(6)[b]	90.45(7)
N(7)–Co(1)–N(6)[b]	89.55(7)	N(7)[a]–Co(1)–N(6)[c]	89.55(7)
N(7)–Co(1)–N(6)[c]	90.45(7)	N(6)[b]–Co(1)–N(6)[c]	180.00
N(7)[a]–Co(1)–N(1)	89.52(7)	N(7)–Co(1)–N(1)	90.48(7)
N(6)[b]–Co(1)–N(1)	95.32(6)	N(6)[c]–Co(1)–N(1)	84.68(6)
N(7)[a]–Co(1)–N(1)[a]	90.48(7)	N(7)–Co(1)–N(1)[a]	89.52(7)
N(6)[b]–Co(1)–N(1)[a]	84.68(6)	N(6)[c]–Co(1)–N(1)[a]	95.32(6)
N(1)–Co(1)–N(1)[a]	180.00	C(8)–Se(1)–C(7)	97.04(10)

Symmetry transformations used to generate equivalent atoms: [a] $-x+2, -y+2, -z$; [b] $-x+1, -y+2, -z$; [c] $x+1, y, z$; [d] $x-1, y, z$.

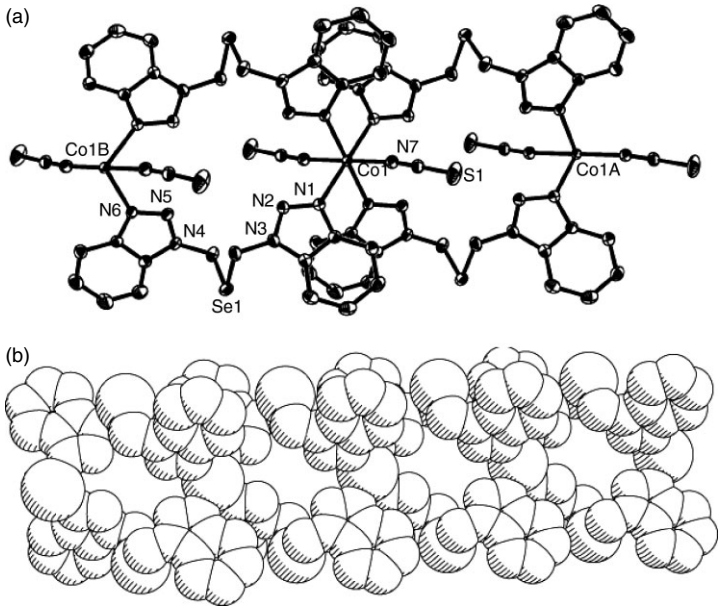

Figure 3. (a) Molecular structure of complex 1. Hydrogen atoms are omitted for clarity. (b) The double-stranded chain of 1.

four equatorial nitrogen atoms from L^{Se} molecules form a parallel quadrilateral, whereas the Co ions lie in the centers of these parallel quadrilaterals [N(1)–Co(1)–N(1) = 180°, N(6)–Co(1)–N(6) = 180°]. The two SCN groups are vertical to the mean plane with 180° of N(7)–Co(1)–N(7) bond angle. Each ligand bridging links two Co(II) centers in a μ-*N*,*N* bidentate fashion. Two L^{Se} and two Co atoms form a 20-membered ring by the coordinated bonds. The Se atoms of L^{Se} are uncoordinated to the metal centers and keep *exo* orientation. The selected bond distances and angles of **1** are summarized in Table 2.

Two strands of ligand are wrapped between each other, and held together by cobalt(II) atoms to present an infinite one-dimensional double-stranded chain. The

Copyright © 2007 John Wiley & Sons, Ltd.

DOI: 10.1002/aoc

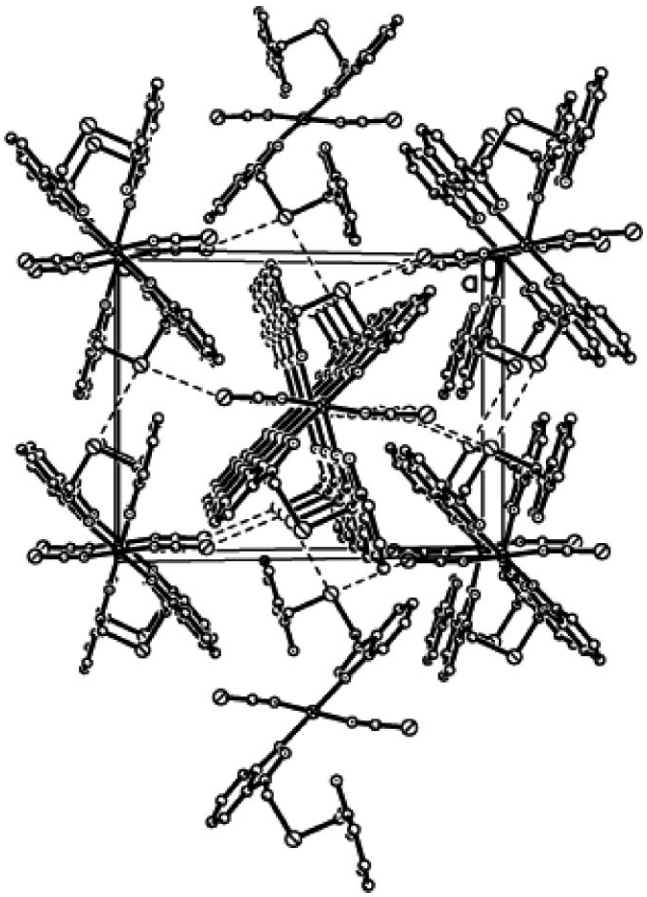

Figure 4. Perspective view of molecular stacking of **1** by the weak molecular interaction between adjacent chains.

Co···Co separation across the bridging ligand in the double-strand chain is 8.822 Å, and the torsion angles, C(8)–Se(1)–C(7)–N(3) and C(7)–Se(1)–C(8)–N(4) is −91.33(17)° and −80.41(17)°, respectively. A rhombic network with a size of 6.243 × 6.475 Å is formed, which is twisted to generate enclosed cavities and no solvent molecules are included in the cavities [Fig. 3(b)]. There are weaker interactions of Se–Se with 3.856 Å and Se–S_{NCS} with 3.608 Å between adjacent chains (Fig. 4).

SOD activities of L^{Se} and complex 1

The autoxidizing velocity of pyrogallol, r_0, can be obtained from Fig. 5. The autoxidation of pyrogallol after adding L^{Se} with various concentrations is shown in Fig. 6, and the autoxidation velocities of pyrogallol with various concentrations of L^{se}, r_i, are summarized in Table 3. It is obvious that the greater the concentration of L^{Se}, the lower the velocity of pyrogallol autoxidizing, which shows that the inhibition of L^{Se} to superoxide anion is increasing with increasing concentration of L^{Se} added. The inhibition rate (η)is calculated by the formula: $\eta = 1 - r_i/r_0$.

The inhibition rate vs concentration of L^{Se} is shown in Figure S2 (see Supplementary Material). The IC_{50} of L^{Se} can be obtained from Figure S2. The IC_{50} value exerts the SOD activity equivalent to one unit of native SOD. The IC_{50} value of L^{Se} is 42 μg ml^{-1} (118.69 μmol dm^{-3}),

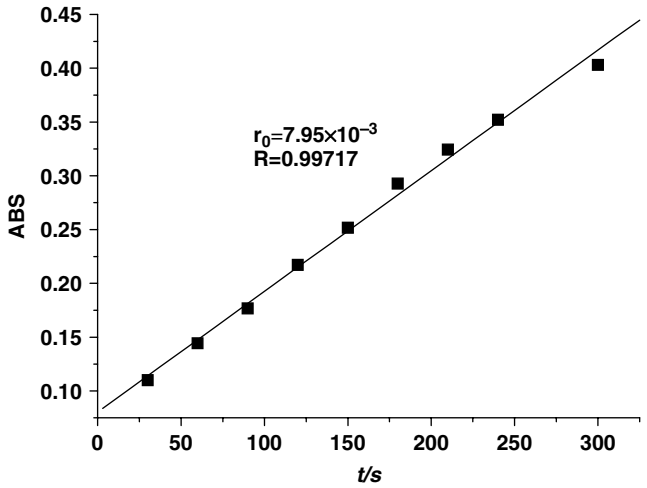

Figure 5. The velocity of self-oxidizing of pyrogallol.

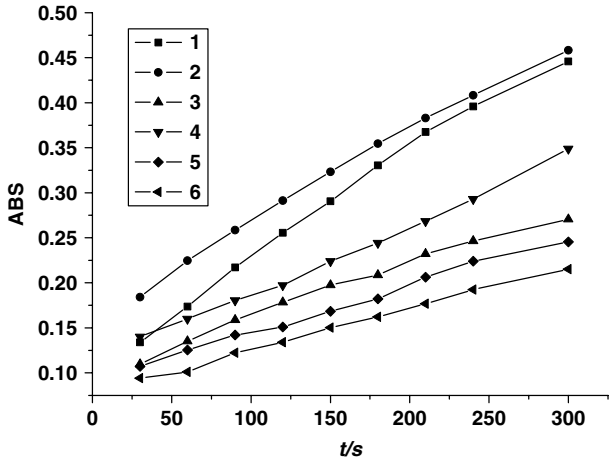

Figure 6. The plots on the absorption (*A*) of pyrogallol by the action of L^{Se} with various concentrations vs time (s). The concentration of L^{Se} added in 1, 2, 3, 4, 5 and 6 samples is 2, 8, 20, 30, 40, 50 μg ml^{-1}, respectively.

Table 3. The inhibition of L^{Se} to the autoxidation of pyrogallol

No. of sample	Concentration (μg ml^{-1})	r_i (10^{-3})	η (%)
1	2	9.97	—
2	8	7.53	5.283
3	20	6.67	16.101
4	30	5.17	34.969
5	40	4.15	47.799
6	50	2.76	65.283

Copyright © 2007 John Wiley & Sons, Ltd.

DOI: 10.1002/aoc

Table 4. The absorption data of pyrogallol including **1** with various concentrations in various times (s), and that of the autoxidation of pyrogallol for comparison[a]

		Running time (s)								
No. sample	C μg cm^{-3}	10	20	30	40	50	60	70	80	90
1	20	0.074	0.131	0.185	0.249	0.295	0.337	0.364	0.404	0.441
2	30	0.076	0.166	0.241	0.309	0.364	0.410	0.454	0.496	0.525
3	40	0.081	0.192	0.280	0.344	0.391	0.430	0.469	0.476	0.483
4	50	0.176	0.308	0.393	0.460	0.506	0.545	0.574	0.598	0.612
5	60	0.179	0.254	0.309	0.347	0.384	0.416	0.424	0.435	0.611
pyrogallol	5.94	0.085	0.098	0.110	0.123	0.132	0.144	0.154	0.166	0.177

[a] The absorption data of the samples are the average of three measurements.

which indicates that the compound L^{Se} has potent SOD activity. To ascertain the SOD activity of the new ligand, we compared the IC_{50} value with those of transition metal complexes as SOD models from references. It is obvious that the IC_{50} of L^{se}, 40 μg ml^{-1} (118 μmol dm^{-3}), is better than that (IC_{50} = 53 μg ml^{-1}) of Co(phenyl-sulfonyl-amide) in the detecting method used by Qiao *et al*.,[23] and it is also close to that [IC_{50} = 105 μmol dm^{-3}]of the Mn(DEF) in the detecting cytochrome C assay by Faulkner *et al*.[24]

The procedures of the inhibition of complex **1** to the autoxidation of pyrogallol are the same as those of L^{Se}. The results are summarized in Table 4.

From Table 4, we can see that there is basically no inhibition role in the autoxidation of pyrogallol for complex **1**. Only numbers 1–3 show slight inhibition before 10 s reaction. The absorptions increase with increasing reaction time and the concentration of **1** added, which might be due to the generation of some color species. The results show that the metal ion might catalyze the generation of the color unknown species, so that the absorptions increase rapidly.[25]

Thermal properties of complex 1

Polymeric complex **1** was heated from room temperature to 800 °C under N_2. TGA results indicate that the framework structure of **1** is stable up to 260 °C and then it decomposed rapidly. The residual weight of 22.54% corresponds to the percentage (26.58%) of Co, Se and S components, indicating that the final product is CoS and CoSe.

Luminescent properties of complex 1

The emission spectra of complex **1** in solid state at room temperature are shown in Figure S1 (see Supplementary data). Excitation at 420 nm leads to blue-light fluorescent emission broad band at 472 nm, assigned to the ligand-to-metal charge transfer (LMCT), which is red-shifted compared with the free ligand (λ_{em} = 360 nm).

CONCLUSIONS

A new ligand, Se (CH_2-*N*-Btrzole)$_2$ (L^{se}) and its cobalt(II) complex [Co(L^{se})$_2^{\bullet}$(SCN)$_2$] (**1**) have been synthesized and characterized. Single crystals of L^{Se} reveal a meso-configuration with a symmetric plane through the central Se atom, the intermolecular weak interactions of Se–Se, Se–N and $\pi-\pi$ stacking between benzotriazole rings to extend the molecular structure to two-dimensional network configuration. The cobalt(II) complex is a six coordinated octahedron. Two Co(II) are linked by two L^{Se} to form a 20-membered macrocycle; the adjacent macrocycles are linked by coordinated bond of Co–$N_{btrizole}$ to extend an infinite double strained chain. The SOD activity of the ligand and Co(II) complex have been studied by pyrogallol autoxidation method. The results show that L^{Se} presents very good inhibition to autoxidation of pyrogallol due to inclusion of the Se component, while the inhibition is not obvious for the cobalt(II) complex, in which there might be some color species generated to interrupt the inhibition.

Supplementary materials

Crystallographic data for structural analysis of L^{Se} and complex **1** have been deposited with Cambridge Crystallographic Data Centre, CCDC 282 496 for Co(II) complex and CCDC 285 072 for L^{Se}, respectively. These data can be obtained free of charge on application to CCDC, 12 Union Road, Cambridge CB2 1EZ, UK (Fax: +44 1223 336 033; e-mail: deposit@ccdc.cam.ac.uk or www: http://www.ccdc.cam.ac.uk). Figure S1 [Emission spectra of **1** in the solid state at room temperature (λ_{ex} = 420 nm)] and Figure S2 (SOD activity of L^{Se} in pyrogallol self-oxidizing assay).

REFERENCES

1. Back TG, Mousa Z, Parvez M. *J. Org. Chem.* 2002; **67**: 499.
2. Wirth T. *Angew. Chem.* 2000; **112**: 3890.
3. Writh T. *Organoselenium Chemistry*. Springer:Berlin, 2000; Vol. 208.
4. Chasteen TG, Bentley R. *Chem. Rev.* 2003; **103**: 1.
5. Mugesh G, du Mont WW, Sies H. *Chem. Rev.* 2001; **101**: 2125.

Copyright © 2007 John Wiley & Sons, Ltd.

DOI: 10.1002/aoc

6. Commandeur JN, Rooseboom M, Vermeulen NP. *Adv. Exp. Med. Biol.* 2001; **500**: 105.
7. Singh HB, Sudha N. *Polyhedron* 1996; **15**: 745.
8. Arnold J. In *Progress in Inorganic Chemistry*, Karlin KD (ed.). Wiley: New York, 1995; Vol. 43; 353–418.
9. Gleizes AN. *Chem. Vap. Depos.* 2000; **6**: 155.
10. Bochmann M. *Chem. Vap. Depos.* 1996; **2**: 85.
11. Lazell M, O'Brien P, Otway DJ, Park JH. *J. Chem. Soc., Dalton Trans.* 2000; 4479.
12. Bhasin KK, Arora V, Sharma SK, Venugopalan P. *Appl. Organometal. Chem.* 2005; **19**: 161.
13. Chang Q, Meng XR, Song YL, Hou HW. *Inorg. Chim. Acta* 2005; **358**: 2117.
14. Lobbia GG, Pellei M, Pettinari C, Santini C. *Inorg. Chim. Acta.* 2005; **358**: 3633.
15. Diamantopoulou E, Raptopoulou CP, Terzis A. *Polyhedron* 2002; **21**: 2117.
16. Katritzky AR, Rachwal S, Rachwal B. *J. Org. Chem.* 1989; **54**: 6022.
17. Sheldrick GM. Correction Software, University of Götingen, 1996.
18. Sheldrick GM. SHELXS-97, Program for Crystal Structures, University of Göttingen, 1997.
19. Sheldrick GM. SHELXL 97, Progeram for the Refinement of Crystal Structures, University of Göttingen, 1997.
20. Cheng WM, Zeng LM, Xu JH. *Pharm. J of Chinese People's Liberation Army* 1996; **6**: 14.
21. Mryer EA., Castellano RK, Diederich F. *Angew. Chem. Int. Edn* 2003; **42**: 1210.
22. Borsting P, Steel PJ. *Eur. J. Inorg. Chem.* 2004; 376.
23. Qiao Y-H, Sun M. *Chem. Res. Applic. (Chin.)* 2003; **15**(4): 583.
24. Faulkner KM, Stevens RD, Fridovich I. *Arch. Biochem. Biophys.* 1994; **310**: 341.
25. Marklund S, Marklund G. *Eur. J. Biochem.* 1974; **47**: 469.

Copyright © 2007 John Wiley & Sons, Ltd.

DOI: 10.1002/aoc